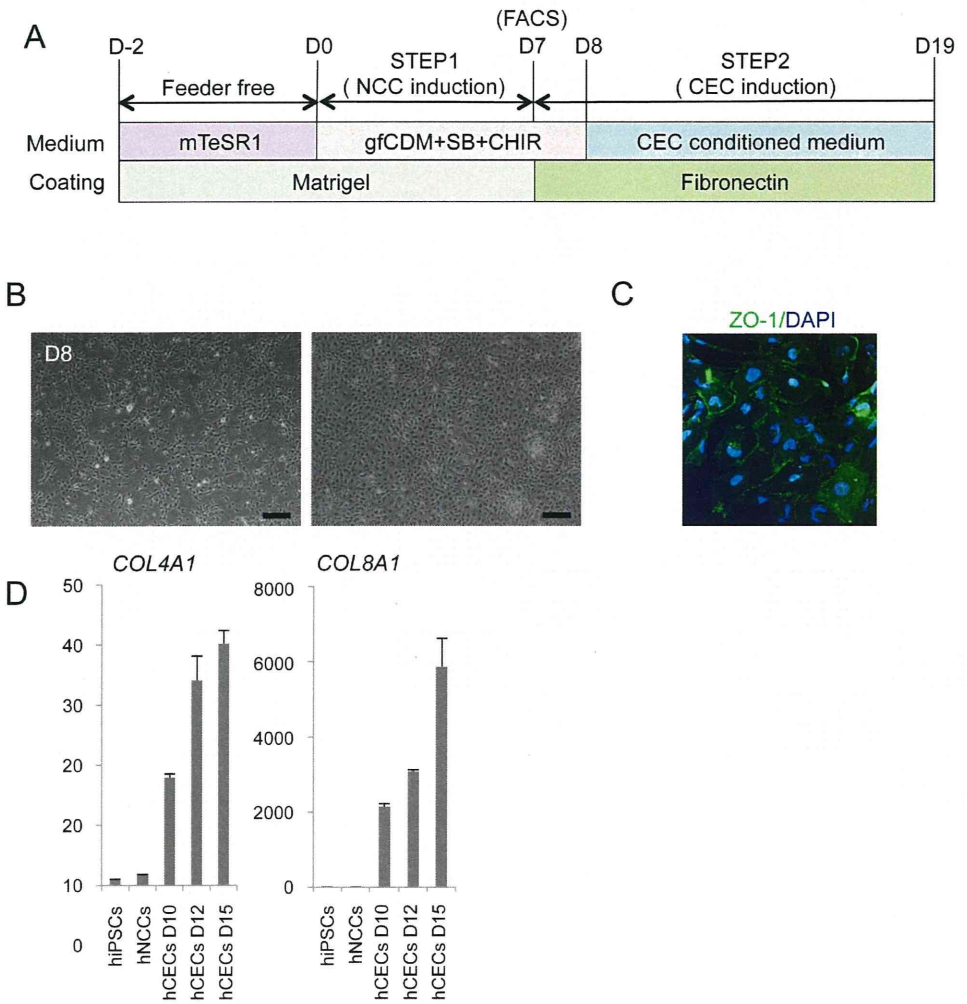

Figure 6. Derivation of corneal endothelial cells from hNCCs. A) Schematic protocol for the induction of corneal endothelial cells. B) Phase contrast images of cells before (D8) and after (D19) the induction. Scale bar, 200 μm. C) The expression of ZO-1 in cells at D12. Cells were stained with an antibody against ZO-1. D) The mRNA expression of corneal endothelial cell marker genes. RNAs were extracted from cells at D10, D12, and D15. The expression level of each gene was demonstrated as a relative value using the value in human primary corneal endothelial cells as 1.0. Average ± SD. N=3, technical triplicate. We performed this CEC induction twice and confirmed its reproducibility.

doi:10.1371/journal.pone.0112291.g006

expression profiles were considerably different, suggesting the protocol-dependent heterogeneity of PSC-derived NCCs.

Sustained expansion of hNCCs with original characteristics

We investigated whether hNCCs could be stably expanded. The growth of hNCCs cultured in the hNCC induction medium (CDM with SB and CHIR) was very slow (data not shown). We employed a cultured condition using CDM supplemented with SB, EGF (20 ng/ml), and FGF2 (20 ng/ml) based on the

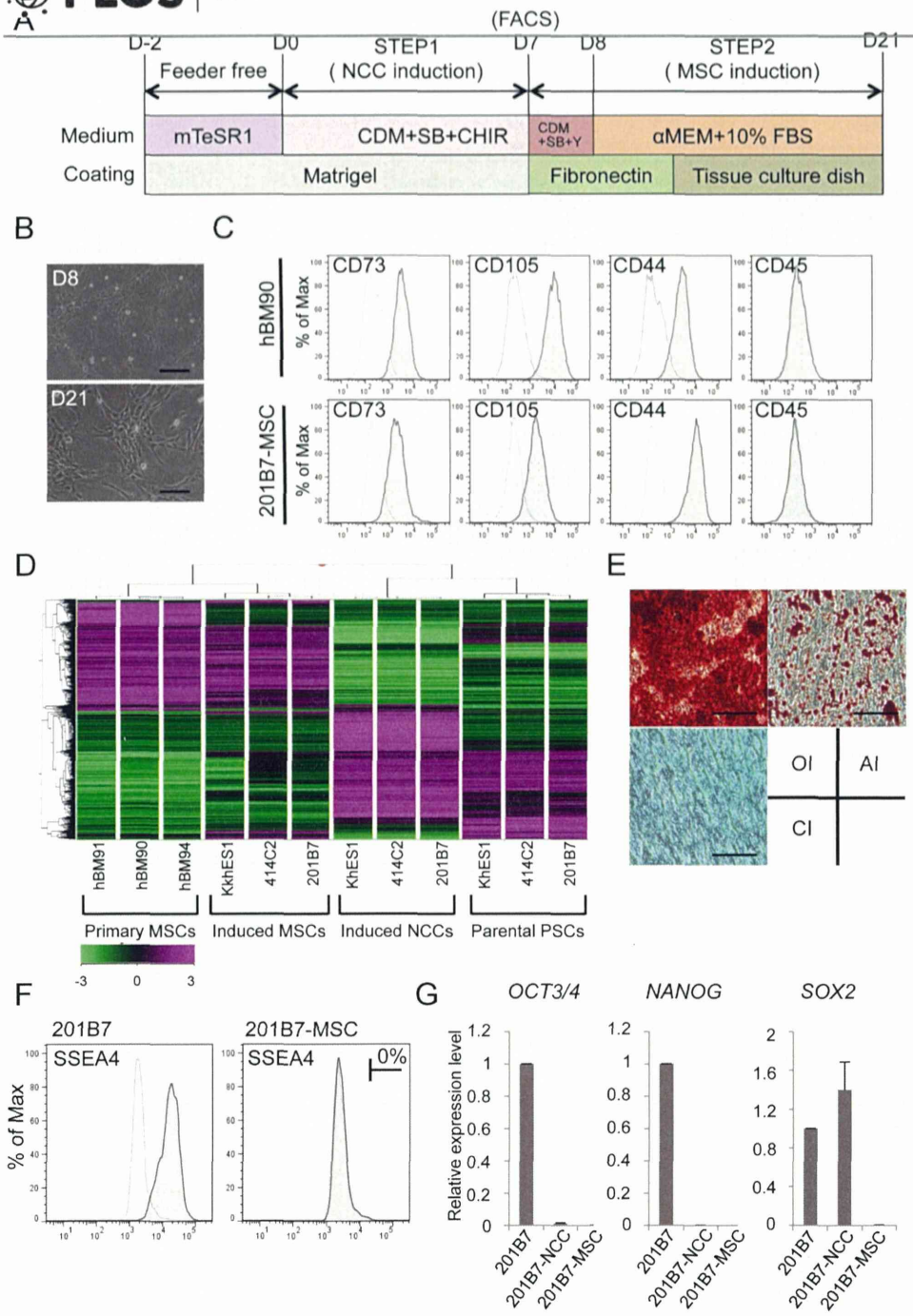

Figure 7. Derivation of hMSCs from hNCCs. A) Schematic protocol for the induction of hMSCs. B) Phase contrast images of cells before (D8) and after (D21) the induction. Scale bar, 200 μm. C) Expression of surface markers in hBM-MSCs (hBM90) and 201B7-derived MSCs (201B7-MSC). D) Hierarchical clustering analyses by genome-wide gene expression profiles. RNAs were extracted from hBM-MSCs (BM90, BM91 and BM94), induced-MSCs, and the corresponding hNCCs and hiPSCs. E) Differentiation properties of induced-MSCs. The induction for osteogenic (OI), chondrogenic (CI), and adipogenic (AI) lineages was performed as described in the Materials and Methods section and evaluated by Alizarin Red staining (OI), Alcian Blue staining (CI), and Oil Red O staining (AI), respectively. Scale bar, 100 μm. F) Population of SSEA4-positive cells. G) The expression levels of pluripotent markers (*OCT3/4*, *NANOG* and *SOX2*) in hPSCs, hNCCs, and hMSCs. Average ± SD. N=3, biological triplicates.

doi:10.1371/journal.pone.0112291.g007

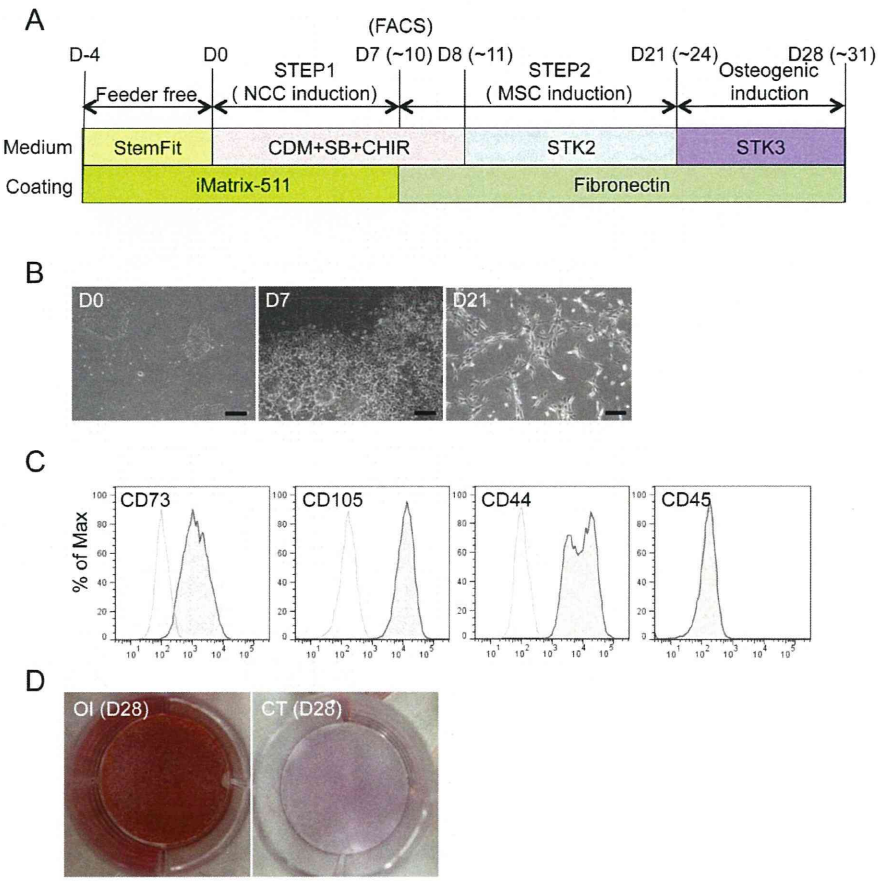

Figure 8. Derivation of hMSCs from hNCCs under defined culture conditions. A) Schematic protocol for the induction of hMSCs from hNCCs under defined culture conditions. B) Phase contrast images of cells 0, 7, and 21 days after the hNCC and hMSC induction, respectively. Scale bar, 200 μm. C) Expression of hMSC-related surface markers in hMSCs induced under defined culture conditions. D) Osteogenic differentiation (OI) properties of hMSCs induced under defined culture conditions. hMSCs were cultured during the induction period in STK2 as a control.

doi:10.1371/journal.pone.0112291.g008

findings of previous studies [33], and consequently observed marked improvements in growth and the stable proliferation of hNCCs even after 10 passages (Figures 3A, B). The expanded hNCCs maintained their original cell morphology and all cells expressing NCC markers, such as TFAP2A (Figure 3C). The global gene expression profiles of hNCCs after prolonged expansion (PN10) were similar to those of early-passage cells (PN0) (Figure S4A and S4B, correlation coefficient =0.96 to 0.98) and markedly different from those of original hPSCs (Figures 3D and S4C).

Modulation of the characteristics of hNCCs by insulin and retinoic acid (RA)

The results of the microarray analyses revealed that induced hNCCs expressed some genes characteristic to cranial NCCs (high for *OTX2* and *DLX1*; low for *HOXA2* and *HOXA3*) (date not shown). A previous study demonstrated that the depletion of insulin from CDM (growth-factor free CDM; hereafter referred to as gfCDM) induced a more anterior neuroectoderm (rostral hypothalamic progenitor-like cells), while retinoic acid (RA) exhibited posteriorizing activity [15]. Therefore, we compared the expression of regional markers in hNCCs cultured with gfCDM, CDM, and CDM with RA (100 nM) (Figure 4A). As expected, the expression of *OTX2*, a marker for mesencephalic NCCs (Figure 4B) [34], was slightly higher under the gfCDM condition than under the CDM condition (Figure 4C). The *DLX1* gene, a marker for first and second branchial arch NCCs (Figure 4B) [35], was expressed in cells cultured under all conditions, and was the highest in CDM with the RA condition (Figure 4C). The expression of the *HOXA2* and *HOXA3* genes, which are markers of the second and third branchial arches, was negligible under the gfCDM and CDM conditions (Figures 4B, C) [36, 37]. Taken together, these results indicated that the regional identities of hNCCs could be modulated by exogenous signals including insulin and RA.

Derivation of peripheral neurons, glia, and melanocytes from hNCCs

We next examined the differentiation potentials of induced hNCCs. Neuronal differentiation was initiated by sphere formation and promoted by culture media containing a mixture of factors (BDNF, GDNF, NGF, and NT-3). Cells expressed β-tubulin and peripherin after 14 days, which indicated differentiation into peripheral neurons (Figure 5A). Further cultivation under the same conditions (4 to 6 weeks) promoted the glial differentiation of hNCCs (Figure 5B).

Melanocytes are well-known derivatives of NCCs. Using a previously described method that included CHIR, EDN3, and BMP4 [15, 38], induced hNCCs expressed microphthalmia-associated transcription factor (*MITF*) and *c-KIT*, markers for melanocytes (Figure 5C). These differentiation properties were compatible with those of NCCs *in vivo*.

Derivation of corneal endothelial cells from hNCCs

Cranial NCCs have been shown to exhibit the ability to differentiate into corneal endothelial cells *in vivo* [39, 40]. Therefore, we examined whether hNCCs grown in gfCDM, which preferentially expressed more anterior NCC markers (Figures 4B, C), could differentiate into cells harboring the characteristics of corneal endothelial cells. When 201B7-derived hNCCs were cultured in the conditioned medium of corneal endothelial cells for twelve days (Figure 6A), cells changed their morphology into that of polygonal corneal endothelial-like cells (

Figure 6B) and started to express the corneal endothelial marker, ZO-1 (Figure 6C). Descemet's membrane is known to consist of collagen type 4 and collagen type 8, which are derived from the corneal endothelium [41]. The mRNA expression of the *COL4A1* and *COL8A1* genes was confirmed in induced endothelial-like cells (Figure 6D). These results strongly suggested that the hNCCs induced in this study possessed the characteristics of cranial NCCs, which exhibit the potential to differentiate into cranial NCC-derived structures.

Derivation of hMSCs from hNCCs

Cranial NCCs also have differentiation properties toward mesenchymal cells, which construct the cranio-facial skeleton, and may be referred as MSCs [3]. In order to derivate hMSCs from hNCCs, the culture medium was changed from that for hNCC to αMEM with 10% FBS (Figure 7A), which we used previously for human bone marrow-derived MSCs (hBM-MSCs) [24]. Through the induction of hMSCs, the expression of *NGFR* and *SOX10* reduced rapidly within 48 hours (PN0) of the medium change, while that of *PAX3* and *TFAP2A* reduced gradually until passage 3 (Figure S5A). Conversely, the expression of MSC markers (*CD73*, *CD105*, and *CD44*) increased rapidly within 48 hours, reached a maximum by passage number 2, and maintained their expression at a level comparable to that in BMMSCs (Figure S5B). These results indicated that the transition from NCCs to MSCs was gradual during passage number three. Cells passaged three times in the medium showed a typical fibroblastic morphology similar to that of hMSCs (Figure 7B), and expressed surface markers for hMSCs (positive for CD73, CD105, and CD44, and negative for CD45) (Figure 7C). Microarray analyses revealed that hNCC-derived MSCs had a global expression pattern similar to that of primary hBM-MSCs (Figure 7D). Differentiation properties toward osteogenic, chondrogenic, and adipogenic lineages are one of the criteria required for MSCs [42], which were clearly confirmed in hNCC-derived MSCs (Figure 7E). FACS analysis showed that there was no SSEA4-positive cells (Figure 7F) and the expression of PSC marker genes was below detectable levels (Figure 7G).

Derivation of osteogenic cells from hiPSCs under defined culture conditions

We determined the feasibility of inducing terminally differentiated cells from iPSCs under defined culture conditions (Figure 8). 987A3 hiPSCs were used as the initial material, which have been generated and maintained under feeder-free and xeno-free conditions [21]. Cells were dissociated into single cells, seeded on iMatrix-coated dishes (0.83–1.35 cells/cm^2), and cultured with StemFit medium for five days. hNCCs were then induced for seven to ten days (Figure 8A). The efficiency of hNCC induction under these conditions was 40.9 $\pm$ 5.5% ($\pm$ SD. N=3, biological triplicate). The induction of hMSCs was performed using CDM for MSCs (STK2) instead of αMEM/10% FBS (Figure 8A). After several passages of hNCCs in STK2, the morphology of cells changed from cuboidal to fibroblastic,

similar to that of hBM-MSCs (Figure 8B). The expression patterns of surface markers were compatible with those of hMSCs (positive for CD73, CD105, and CD44, and negative for CD45) (Figure 8C) and the differentiation properties for osteogenic, chondrogenic, and adipogenic lineages were confirmed when the standard FBS-containing induction medium was used (Figure S6). Osteogenic differentiation was also confirmed using the chemically-defined osteogenic medium (STK3) (Figure 8D). These results indicated that all steps from iPSC to osteogenic cells could be performed under defined culture conditions.

Discussion

In the present study, we developed a simple and efficient induction method for hNCCs from hPSCs. The induction efficiency of this method was high (70–80%) irrespective with the type of hPSC. The induced hNCCs exhibited the cranial NCC characters under maintenance culture conditions, while further treatment with insulin and RA marginally posteriorized hNCCs. Consistent with the expression of cranial NCC markers, induced hNCCs could differentiate into corneal endothelial cells, which is a characteristic of cranial NCCs.

Our protocol was independent of the BMP signal. In our protocol, DMH1, a specific BMP inhibitor, clearly attenuated the induction efficiency of the $p75^{high}$ fraction (Figure S1). This result clearly contradicted the findings of previous studies (no effect [14] or increased efficiency [15]). The marked differences in the findings of these studies may be attributed to the seeding density used at the beginning of induction. The seeding density of our protocol was approximately 2–4 clumps/cm^2 (approximately 20 cells/cm^2), while other studies used 1×10^4 cells/cm^2 [26]. Both CNS and neural crest fates were previously observed when cells were seeded at a low density, while CNS cells primarily formed at a high density [43]. In accordance with these findings, the efficiency of the NCC induction was markedly decreased if clumps were seeded at a higher density (data not shown). The high density of hNCCs may have exaggerated local BMP signaling secreted from the hNCCs themselves. Therefore, we combined high density seeding with the BMP inhibitor treatment; however, the efficiency was still low (data not shown). Based on these results, we could not account for the differences between our protocol and those of previous studies.

In order to compare the hNCCs in this study with those in previous studies, we analyzed gene expression profiles of hNCCs published previously. The comparison of the relative induction levels of NCC specific genes revealed that hNCCs differentiated by our protocol and previous studies showed similarities in some aspects, but overall profiles were different from each other (Figure S3). These results indicated that induction protocols reported in this study and in the previous studies induced different subset of hNCCs.

Induced hNCCs exhibited differentiation properties for multiple cell lineages including peripheral neurons, glial cells, melanocytes, and corneal endothelial cells, and also delivered hMSCs that further differentiated into osteogenic,

chondrogenic, and adipogenic cells. These properties are compatible with NCCs being multipotent stem cells [3]. However, clonal analyses are indispensable for confirming the stemness of induced hNCCs. Previous clonal analyses revealed that 63–65% of the hNCC clones could differentiated into multi-lineage cells positive for markers of neurons, glial cells, and smooth muscle cells [43, 44], suggesting that hNCCs induced from hPSCs were multipotent on the clonal level. Although stemness has yet to be investigated in this study, induced hNCCs in this protocol will be a promising cell source for various types of research.

Human diseases that have been related to the development of hNCCs include Hirschsprung's disease, DiGeorge syndrome, Waardenburg syndrome, Charcot-Marie-tooth disease, Hermansky-Pudlak syndrome, familial dysautonomia, Chediak-Higashi syndrome, and CHARGE syndrome [45, 46]. hNCCs containing the mutations responsible for these diseases can be induced from hiPSCs established from the respective patients; therefore, this will be a powerful tool for creating *in vitro* disease models that can contribute to a more detailed understanding of the pathogenesis of NCC disorders and also to the development of novel therapeutic modalities [15]. In addition, hNCCs have been shown to be the cell-of-origin of some cancers such as neuroblastoma [47], which indicates that hNCCs can be used in *in vitro* transformation experiments. We have already confirmed that the survival rate of freeze-stocked hNCCs was satisfactory and the freeze and thaw process had no impact on the growth and differentiation properties of these cells (data not shown). These are favorable features for a material in research because it is important to use cells of the same quality in order to evaluate reproducibility.

Induced hNCCs-deridatives can also be used for cell therapy. In this regard, hNCC-derived hMSCs will be a very useful material. hMSCs have been used in a wide range of regenerative medicines, and promising results have been reported in some cases [48, 49]. In contrast with the advances reported in clinical applications, many issues related to the biology of hMSCs have yet to be investigated, one of which is the cell-of-origin of hMSCs. hNCCs may be the precursors of hMSCs based on the finding that craniofacial skeletal tissues are derived from NCCs [50]. This has also been supported in lineage tracing experiments using P0-cre mice [51, 52]. Current sources of hMSCs include bone marrow, fat tissue, synovium, and umbilical cord; however, it remains unclear whether NCC-derived cells exist in all of these adult tissues and serve as the source of hMSCs. A comparison between hNCC-derived MSCs and somatic tissue-derived hMSCs may provide more information related to this issue.

One of the limitations of current hMSCs is their limited proliferative activity, which may pose problems in their application to conditions requiring a large amount of cells. This can be overcome if hNCC-derived MSCs are used because hNCCs can be induced from hPSCs, which have unlimited proliferative activity. Two issues are important for this application. One is to be free from infectious substances that may be derived from animal materials. Using iPSCs generated and maintained under feeder-free and xeno-free conditions, we successfully induced hNCCs and hMSCs with minimum animal material (BSA in CDM) (Figure 8A).

Furthermore, we generated terminally differentiated cells (osteogenic cells) from these MSCs under chemically defined media. To the best of our knowledge, this is the first study to demonstrate the induction of osteogenic cells under feeder-free and serum-free conditions from PSCs. The other concern relates to the contamination of undifferentiated cells, particularly parental hPSCs, which may lead to serious conditions such as the formation of malignant tumors [53]. We confirmed that hNCC-derived hMSCs were free from SSEA4-expressing cells and the expression of PSC-marker genes was below detectable levels (Figures 7F, G). Although more precise and meticulous analyses are required to prove the safety of these cells, the results of the present study have provided evidence to promote the use of hNCC-derived hMSCs for cell therapy.

Supporting Information

Figure S1. Effect of the BMP signal on the induction of $p75^{high}$ cells. hiPSCs (201B7) were treated in NCC induction media with BMP4 (10 ng/ml) (A) or DMH1 (10 μM) (B), and the fraction of p75-positive cells was analyzed by FACS. C) Effects of BMP signal inhibitors on the induction of $p75^{high}$ cells. 201B7 cells were treated with each BMP inhibitor at the indicated dosage, and the fraction of p75-positive cells was analyzed by FACS.
doi:10.1371/journal.pone.0112291.s001 (TIFF)

Figure S2. Global comparison of the expressions of genes between PSCs and $p75^{high}$ cells. A) A volcano plot showing the P value for differences in the expression of each gene between the average of PSC lines (H9, KhES1, 414C2, and 201B7) and the average of corresponding $p75^{high}$ cells. A total of 562 entities downregulated and 447 entities upregulated in $p75^{high}$ cells were identified as a differentially expressed gene set. B) Heat map analyses revealed global similarities among hNCCs derived from each PSC line.
doi:10.1371/journal.pone.0112291.s002 (TIFF)

Figure S3. Expression of NCC marker genes in induced NCCs from PSCs. The induction ratio of NCC markers relative to a corresponding pluripotent baseline was demonstrated in each induced NCC. iPS NCCs, GSE44727. WA09_NC_Day11, 45223. Marker genes for each sub-population of NCC were labeled using the indicated colors.
doi:10.1371/journal.pone.0112291.s003 (TIFF)

Figure S4. Comparison of gene expression profiles between hNCCs at different passages by scatter plotting. RNAs were extracted from hNCCs derived from 201B7 (A) and KhES1 (B) at different passages (PN0, PN4 and PN10), and analyzed using microarrays. C) Correlation coefficient analysis was performed using these data.
doi:10.1371/journal.pone.0112291.s004 (TIFF)

Figure S5. The expression of markers for hNCCs and hMSCs in each passage. A gradual transition from hNCCs to hMSCs was observed in hNCC markers (A)

and hMSC markers (B). Average ± SD. N=3, biological triplicates. Regarding BMSCs, cDNA was prepared from the bone marrow stromal cells of four healthy donors (BM25, 26, 34, and 107), and the average was presented as BMSCs in each graph.
doi:10.1371/journal.pone.0112291.s005 (TIFF)

Figure S6. Osteogenic-, chondrogenic-, adipogenic induction from feeder-free hiPSCs through hNCC-derived hMSCs. Differentiation properties of hNCC-MSCs. The induction for osteogenic (OI), chondrogenic (CI), and adipogenic (AI) lineages was performed as described in the Materials and Methods section and evaluated by Alizarin Red staining (OI), Alcian Blue staining (CI), and Oil Red O staining (AI), respectively. Scale bar, 200 μm.
doi:10.1371/journal.pone.0112291.s006 (TIFF)

Table S1. Information of primary antibodies used in this study.
doi:10.1371/journal.pone.0112291.s007 (TIF)

Table S2. Information of PCR primers used in this study.
doi:10.1371/journal.pone.0112291.s008 (TIF)

Acknowledgments

We thank Dr. H. Tanaka for the kind advice and help in the corneal endothelium induction, M. Shibata, K.R. Komatsu, and J. Nakai for their technical assistance, and T. Kato, Y. Jin. S. Tamaki, and S. Hineno for their support during this study.

Author Contributions

Conceived and designed the experiments: MF NK TN MS TO SK MU MI JT. Performed the experiments: MF YN KK KS SN YM TY NO TS MI. Analyzed the data: MF YN KK NK MU TS MI. Contributed reagents/materials/analysis tools: MN TY KU TH. Wrote the paper: MF YN TY MU MI JT.

References

1. **Liu Z, Tang Y, Lu S, Zhou J, Du Z, et al.** (2013) The tumourigenicity of iPS cells and their differentiated derivates. J Cell Mol Med 17: 782–791.
2. **Le Douarin NM, Dupin E** (2003) Multipotentiality of the neural crest. Curr Opin Genet Dev 13: 529–536.
3. **Sauka-Spengler T, Bronner-Fraser M** (2008) A gene regulatory network orchestrates neural crest formation. Nat Rev Mol Cell Biol 9: 557–568.
4. **Kalcheim C, Burstyn-Cohen T** (2005) Early stages of neural crest ontogeny: formation and regulation of cell delamination. Int J Dev Biol 49: 105–116.
5. **Kalcheim C** (2000) Mechanisms of early neural crest development: from cell specification to migration. Int Rev Cytol 200: 143–196.
6. **Vincent SD, Buckingham ME** (2010) How to make a heart: the origin and regulation of cardiac progenitor cells. Curr Top Dev Biol 90: 1–41.

7. **Neirinckx V, Coste C, Rogister B, Wislet-Gendebien S** (2013) Concise review: adult mesenchymal stem cells, adult neural crest stem cells, and therapy of neurological pathologies: a state of play. Stem Cells Transl Med 2: 284–296.

8. **Neirinckx V, Marquet A, Coste C, Rogister B, Wislet-Gendebien S** (2013) Adult bone marrow neural crest stem cells and mesenchymal stem cells are not able to replace lost neurons in acute MPTP-lesioned mice. PLoS One 8: e64723.

9. **Giuliani M, Oudrhiri N, Noman ZM, Vernochet A, Chouaib S, et al.** (2011) Human mesenchymal stem cells derived from induced pluripotent stem cells down-regulate NK-cell cytolytic machinery. Blood 118: 3254–3262.

10. **Villa-Diaz LG, Brown SE, Liu Y, Ross AM, Lahann J, et al.** (2012) Derivation of mesenchymal stem cells from human induced pluripotent stem cells cultured on synthetic substrates. Stem Cells 30: 1174–1181.

11. **Liu Q, Spusta SC, Mi R, Lassiter RN, Stark MR, et al.** (2012) Human neural crest stem cells derived from human ESCs and induced pluripotent stem cells: induction, maintenance, and differentiation into functional schwann cells. Stem Cells Transl Med 1: 266–278.

12. **Chimge NO, Bayarsaihan D** (2010) Generation of neural crest progenitors from human embryonic stem cells. J Exp Zool B Mol Dev Evol 314: 95–103.

13. **Milet C, Monsoro-Burq AH** (2012) Embryonic stem cell strategies to explore neural crest development in human embryos. Dev Biol 366: 96–99.

14. **Menendez L, Yatskievych TA, Antin PB, Dalton S** (2011) Wnt signaling and a Smad pathway blockade direct the differentiation of human pluripotent stem cells to multipotent neural crest cells. Proc Natl Acad Sci U S A 108: 19240–19245.

15. **Mica Y, Lee G, Chambers SM, Tomishima MJ, Studer L** (2013) Modeling neural crest induction, melanocyte specification, and disease-related pigmentation defects in hESCs and patient-specific iPSCs. Cell Rep 3: 1140–1152.

16. **Suemori H, Yasuchika K, Hasegawa K, Fujioka T, Tsuneyoshi N, et al.** (2006) Efficient establishment of human embryonic stem cell lines and long-term maintenance with stable karyotype by enzymatic bulk passage. Biochem Biophys Res Commun 345: 926–932.

17. **Amit M, Carpenter MK, Inokuma MS, Chiu CP, Harris CP, et al.** (2000) Clonally derived human embryonic stem cell lines maintain pluripotency and proliferative potential for prolonged periods of culture. Dev Biol 227: 271–278.

18. **Okita K, Matsumura Y, Sato Y, Okada A, Morizane A, et al.** (2011) A more efficient method to generate integration-free human iPS cells. Nat Methods 8: 409–412.

19. **Takahashi K, Tanabe K, Ohnuki M, Narita M, Ichisaka T, et al.** (2007) Induction of pluripotent stem cells from adult human fibroblasts by defined factors. Cell 131: 861–872.

20. **McMahon AP, Bradley A** (1990) The Wnt-1 (int-1) proto-oncogene is required for development of a large region of the mouse brain. Cell 62: 1073–1085.

21. **Nakagawa M, Taniguchi Y, Senda S, Takizawa N, Ichisaka T, et al.** (2014) A novel efficient feeder-free culture system for the derivation of human induced pluripotent stem cells. Sci Rep 4: 3594.

22. **Nasu A, Ikeya M, Yamamoto T, Watanabe A, Jin Y, et al.** (2013) Genetically matched human iPS cells reveal that propensity for cartilage and bone differentiation differs with clones, not cell type of origin. PLoS One 8: e53771.

23. **Wataya T, Ando S, Muguruma K, Ikeda H, Watanabe K, et al.** (2008) Minimization of exogenous signals in ES cell culture induces rostral hypothalamic differentiation. Proc Natl Acad Sci U S A 105: 11796–11801.

24. **Colleoni S, Galli C, Giannelli SG, Armentero MT, Blandini F, et al.** (2010) Long-term culture and differentiation of CNS precursors derived from anterior human neural rosettes following exposure to ventralizing factors. Exp Cell Res 316: 1148–1158.

25. **James MJ, Jarvinen E, Wang XP, Thesleff I** (2006) Different roles of Runx2 during early neural crest-derived bone and tooth development. J Bone Miner Res 21: 1034–1044.

26. **Lee G, Chambers SM, Tomishima MJ, Studer L** (2010) Derivation of neural crest cells from human pluripotent stem cells. Nat Protoc 5: 688–701.

27. **Ohta S, Imaizumi Y, Okada Y, Akamatsu W, Kuwahara R, et al.** (2011) Generation of human melanocytes from induced pluripotent stem cells. PLoS One 6: e16182.

28. **Fang D, Leishear K, Nguyen TK, Finko R, Cai K, et al.** (2006) Defining the conditions for the generation of melanocytes from human embryonic stem cells. Stem Cells 24: 1668–1677.

29. **Ju C, Zhang K, Wu X** (2012) Derivation of corneal endothelial cell-like cells from rat neural crest cells in vitro. PLoS One 7: e42378.

30. **Umeda K, Zhao J, Simmons P, Stanley E, Elefanty A, et al.** (2012) Human chondrogenic paraxial mesoderm, directed specification and prospective isolation from pluripotent stem cells. Sci Rep 2: 455.

31. **Okamoto T, Aoyama T, Nakayama T, Nakamata T, Hosaka T, et al.** (2002) Clonal heterogeneity in differentiation potential of immortalized human mesenchymal stem cells. Biochem Biophys Res Commun 295: 354–361.

32. **Kreitzer FR, Salomonis N, Sheehan A, Huang M, Park JS, et al.** (2013) A robust method to derive functional neural crest cells from human pluripotent stem cells. Am J Stem Cells 2: 119–131.

33. **Lee G, Ramirez CN, Kim H, Zeltner N, Liu B, et al.** (2012) Large-scale screening using familial dysautonomia induced pluripotent stem cells identifies compounds that rescue IKBKAP expression. Nat Biotechnol 30: 1244–1248.

34. **Kimura C, Takeda N, Suzuki M, Oshimura M, Aizawa S, et al.** (1997) Cis-acting elements conserved between mouse and pufferfish Otx2 genes govern the expression in mesencephalic neural crest cells. Development 124: 3929–3941.

35. **Qiu M, Bulfone A, Ghattas I, Meneses JJ, Christensen L, et al.** (1997) Role of the Dlx homeobox genes in proximodistal patterning of the branchial arches: mutations of Dlx-1, Dlx-2, and Dlx-1 and -2 alter morphogenesis of proximal skeletal and soft tissue structures derived from the first and second arches. Dev Biol 185: 165–184.

36. **Manley NR, Capecchi MR** (1995) The role of Hoxa-3 in mouse thymus and thyroid development. Development 121: 1989–2003.

37. **Liu Z, Yu S, Manley NR** (2007) Gcm2 is required for the differentiation and survival of parathyroid precursor cells in the parathyroid/thymus primordia. Dev Biol 305: 333–346.

38. **Motohashi T, Aoki H, Yoshimura N, Kunisada T** (2006) Induction of melanocytes from embryonic stem cells and their therapeutic potential. Pigment Cell Res 19: 284–289.

39. **Johnston MC, Noden DM, Hazelton RD, Coulombre JL, Coulombre AJ** (1979) Origins of avian ocular and periocular tissues. Exp Eye Res 29: 27–43.

40. **Trainor PA, Tam PP** (1995) Cranial paraxial mesoderm and neural crest cells of the mouse embryo: co-distribution in the craniofacial mesenchyme but distinct segregation in branchial arches. Development 121: 2569–2582.

41. **Fitch JM, Birk DE, Linsenmayer C, Linsenmayer TF** (1990) The spatial organization of Descemet's membrane-associated type IV collagen in the avian cornea. J Cell Biol 110: 1457–1468.

42. **De Schauwer C, Meyer E, Van de Walle GR, Van Soom A** (2011) Markers of stemness in equine mesenchymal stem cells: a plea for uniformity. Theriogenology 75: 1431–1443.

43. **Lee G, Kim H, Elkabetz Y, Al Shamy G, Panagiotakos G, et al.** (2007) Isolation and directed differentiation of neural crest stem cells derived from human embryonic stem cells. Nat Biotechnol 25: 1468–1475.

44. **Curchoe CL, Maurer J, McKeown SJ, Cattarossi G, Cimadamore F, et al.** (2010) Early acquisition of neural crest competence during hESCs neuralization. PLoS One 5: e13890.

45. **Bajpai R, Chen DA, Rada-Iglesias A, Zhang J, Xiong Y, et al.** (2010) CHD7 cooperates with PBAF to control multipotent neural crest formation. Nature 463: 958–962.

46. **Lee G, Papapetrou EP, Kim H, Chambers SM, Tomishima MJ, et al.** (2009) Modelling pathogenesis and treatment of familial dysautonomia using patient-specific iPSCs. Nature 461: 402–406.

47. **Jiang M, Stanke J, Lahti JM** (2011) The connections between neural crest development and neuroblastoma. Curr Top Dev Biol 94: 77–127.

48. **Caplan AI** (2007) Adult mesenchymal stem cells for tissue engineering versus regenerative medicine. J Cell Physiol 213: 341–347.

49. **Silva NA, Sousa N, Reis RL, Salgado AJ** (2013) From basics to clinical: A comprehensive review on spinal cord injury. Prog Neurobiol.

50. **Helms JA, Schneider RA** (2003) Cranial skeletal biology. Nature 423: 326–331.

51. **Morikawa S, Mabuchi Y, Niibe K, Suzuki S, Nagoshi N, et al.** (2009) Development of mesenchymal stem cells partially originate from the neural crest. Biochem Biophys Res Commun 379: 1114–1119.

52. **Takashima Y, Era T, Nakao K, Kondo S, Kasuga M, et al.** (2007) Neuroepithelial cells supply an initial transient wave of MSC differentiation. Cell 129: 1377–1388.

53. **Cai J, Yang M, Poremsky E, Kidd S, Schneider JS, et al.** (2010) Dopaminergic neurons derived from human induced pluripotent stem cells survive and integrate into 6-OHDA-lesioned rats. Stem Cells Dev 19: 1017-1023.

TISSUE ENGINEERING: Part B
Volume 20, Number 3, 2014

DOI: 10.1089/ten.teb.2014.0105

Current Status of Multipotent Mesenchymal Stromal Cells

Syed R. Husain, PhD,[1] Yoshikazu Ohya, PhD,[2] Junya Toguchida, MD, PhD,[3,4] and Raj K. Puri, MD, PhD[1]

THIS SPECIAL ISSUE of the journal highlights the 16th US-Japan Cellular and Gene Therapy Conference entitled "Potential Application of Multipotent Mesenchymal Stromal Cells" held on the National Institutes of Health Campus on February 28, 2013. The conference was jointly organized by the Center for Biologics Evaluation and Research, US Food and Drug Administration (FDA), and the Ministry of Education, Culture, Sports, Science and Technology, Japan under the US-Japan Cooperative Research Program. The scientific themes of these joint annual meetings are selected based on current advances in the area of cellular and gene therapy. Speakers from Japan and the United States kindly agreed to submit their presentations for this special issue of the journal.

Mesenchymal stem cells (MSCs) (also known as multipotent stromal cells) were first isolated from bone marrow and found capable of regenerating rudiments of bone and supporting hematopoiesis *in vivo*.[1] Plastic adherent populations isolated from bone marrow were found to be functionally heterogeneous and exhibited colony-forming unit fibroblasts made up of undifferentiated stem cells and progenitor cells. These cells were also observed for their multipotency through differentiation into mesenchymal cell types, including osteoblasts, chondrocytes, and adipocytes. Because MSCs are generated from the stromal component of bone marrow, they were later renamed multipotent mesenchymal stromal cells (with the same acronym) to reflect their origin and biological properties.[2]

MSCs are a diverse population of cells with a wide range of potential therapeutic applications, which is evident from the variety of indications currently being investigated in clinical trials. Their potential is based on their inherent biological properties such as plasticity, proliferation, migration, self-renewal, and immunosuppression. A large number of clinical studies have been conducted or are ongoing. The FDA has not yet approved any MSC-based products.

These MSC-based products are complex and heterogeneous. The variability in donor and tissue sources, manufacturing processes, phenotypic cell markers, and bioactivity has the potential to significantly impact the product and prevents a direct comparison of therapeutic protocols. Bone marrow is not the sole source of MSC-based products; current research in the use of umbilical cord or placental tissue and adipose-derived MSC-based products has increased significantly.

In spite of numerous challenges and diversity in MSC-based clinical trial products, MSCs have great potential in the field of regenerative medicine. The articles in this issue highlight the promises and challenges in the manufacturing of MSCs and their use in bone tissue regeneration, cirrhosis treatment, and tissue vascularization.

Disclosure Statement

No competing financial interests exist.

References

1. Friedenstein, A.J., Petrakova, K.V., Kurolesova, A.I., and Frolova, G.P. Heterotopic of bone marrow. Analysis of precursor cells for osteogenic and hematopoietictissues. Transplantation **6,** 230, 1968.
2. Dominici, M., Le Blanc, K., Mueller, I., Slaper-Cortenbach, I., Marini, F., Krause, D., Deans, R., Keating, A., Prockop, D.J., and Horwitz, E. Minimal criteria for defining multipotent mesenchymal stromal cells. The International Society for Cellular Therapy position statement. Cytotherapy **8,** 315, 2006.

Address correspondence to:
Syed R. Husain, PhD
Division of Cellular and Gene Therapies
Food and Drug Administration
Center for Biologics Evaluation and Research
HFM-735
NIH Building 29B
29 Lincoln Drive MSC4555
Bethesda, MD 20892-4555

E-mail: syed.husain@fda.hhs.gov

Received: February 10, 2014
Accepted: February 10, 2014
Online Publication Date: March 28, 2014

[1]Division of Cellular and Gene Therapies, Food and Drug Administration, Center for Biologics Evaluation and Research, Bethesda, Maryland.
[2]Department of Integrated Biosciences, Graduate School of Frontier Sciences, University of Tokyo, Kashiwa, Japan.
[3]Department of Tissue Regeneration, Institute for Frontier Medical Sciences, Kyoto University, Kyoto, Japan.
[4]Department of Cell Growth and Differentiation, Center for iPS Cell Research and Application, Kyoto University, Kyoto, Japan.

Biochemical and Biophysical Research Communications 443 (2014) 1014–1020

Contents lists available at ScienceDirect

Biochemical and Biophysical Research Communications

journal homepage: www.elsevier.com/locate/ybbrc

Osteogenic lineage commitment of mesenchymal stem cells from patients with ossification of the posterior longitudinal ligament

Yoshifumi Harada [a,b], Ken-Ichi Furukawa [a,*], Toru Asari [b], Shunfu Chin [a,b], Atsushi Ono [b], Toshihiro Tanaka [b], Hiroki Mizukami [c], Manabu Murakami [a], Soroku Yagihashi [c], Shigeru Motomura [a], Yasuyuki Ishibashi [b]

[a] Department of Pharmacology, Hirosaki University Graduate School of Medicine, 5 Zaifu-cho, Hirosaki 036-8562, Japan
[b] Department of Orthopaedic Surgery, Hirosaki University Graduate School of Medicine, 5 Zaifu-cho, Hirosaki 036-8562, Japan
[c] Department of Pathology and Molecular Medicine, Hirosaki University Graduate School of Medicine, 5 Zaifu-cho, Hirosaki 036-8562, Japan

ARTICLE INFO

Article history:
Received 6 December 2013
Available online 19 December 2013

Keywords:
Spinal ligament
Ossification of the posterior longitudinal ligament
Mesenchymal stem cells
Osteogenic differentiation
Ectopic ossification
Pathogenesis

ABSTRACT

Ectopic bone formation is thought to be responsible for ossification of the posterior longitudinal ligament of the spine (OPLL). Mesenchymal stem cells (MSCs) were isolated from spinal ligaments and shown to play a key role in the process of ectopic ossification. The purpose of this study was to explore the capacity of these MSCs to undergo lineage commitment and to assess the gene expression changes between these committed and uncommitted MSCs between OPLL and non-OPLL patients. Spinal ligament-derived cells were obtained from OPLL patients or patients with cervical spondylotic myelopathy (non-ossified) for comparison ($n = 8$ in each group). MSCs from the two patient cohorts were evaluated for changes in colony forming ability; osteogenic, adipogenic and chondrogenic differentiation potential; and changes in gene expression following induction with lineage-specific conditions. We show that the osteogenic differentiation potential was significantly higher in MSCs from OPLL patients than in those from non-OPLL patients. In addition, alkaline phosphatase activity and several osteogenic-related genes expressions (bone morphogenetic protein 2, runt-related transcription factor 2 and alkaline phosphatase) were significantly higher in the OPLL group than in the non-OPLL group. However, single cell cloning efficiency, adipogenic and chondrogenic differentiation, and the expression of adipogenic and chondrogenic-related genes were equivalent between MSCs harvested from OPLL and non-OPLL patient samples. These findings suggest an increase in the osteogenic differentiation potential of MSCs from OPLL patients and that this propensity toward the osteogenic lineage may be a causal factor in the ossification in these ligaments.

1. Introduction

The posterior longitudinal ligament of the spine lies adjacent to the posterior aspect of the vertebral bodies. Ossification of this ligament is characterized by ectopic bone formation, and is frequently linked with similar ossification in other surrounding spinal ligaments. These ossified lesions often enlarge with time and compress the spinal cord and its roots, leading to neurological deficiencies and a high risk of spinal cord injury [1,2]. Patients with severe symptoms are considered definitive candidates for surgical treatment such as spinal decompression [3]. However, it is worth noting that there are no therapies for preventing the formation and progression of ossified lesions.

Given that some patients have a familial history of OPLL, it is quite possible that genetic factors are partly responsible for this pathogenic condition. The genetic factors pertaining to OPLL are described as multifactorial genetic inheritance [4] and the genes playing a key role in its onset remain unclear. In OPLL patients, ectopic ossification occurs throughout the spine, frequently involving ossification of other spinal ligaments. Consequently, OPLL has been regarded as one of the manifestations of diffuse idiopathic skeletal hyperostosis (DISH) [5,6]. Based on genetic factors, these current findings may indicate that OPLL patients would have a tendency toward systemic ossification of numerous ligaments, similar to that observed in patients with DISH.

Mesenchymal stem cells (MSCs) have been isolated from various tissues and are thought to play essential roles in supplying damaged tissues with a source of progenitor cells for repair. However, several studies have discussed the undesirable effects of MSCs in pathogenic conditions such as fibrodysplasia ossificans progressiva (FOP) [7], ectopic ossification following burn injury [8] and aortic valve calcification [9]. We have focused our attention on the roles of MSCs in the process of ectopic ossification in spinal ligamentous tissues. As a first step, we isolated MSCs from human spinal ligaments and performed immunophenotypic analysis of

* Corresponding author. Fax: +81 172 39 5022.
E-mail address: furukawa@cc.hirosaki-u.ac.jp (K.-I. Furukawa).

0006-291X/$ - see front matter © 2013 Elsevier Inc. All rights reserved.
http://dx.doi.org/10.1016/j.bbrc.2013.12.080

cell surface markers [10]. Furthermore, we previously demonstrated the localization of MSCs in ossified human spinal ligaments [11]. Chondrocytes near the ossification front in ossified spinal ligaments are positive for MSC marker expression, and there is an increase in the prevalence of MSCs in the collagenous matrix near the ossified spinal ligament. Therefore, we suspect that MSCs play a key role in the ectopic ossification process of spinal ligaments. This study was aimed to explore the capacity of MSCs to undergo lineage commitment and to determine the gene expression changes that occur in committed and uncommitted MSCs and how this differs between OPLL and non-OPLL patients.

2. Materials and methods

2.1. Samples

The study was approved by the Committee of Medical Ethics of Hirosaki University Graduate School of Medicine. All patients gave written informed consent to participate. Ligamentum flava at the C3 level were collected aseptically during surgery of the cervical spine from eight patients with OPLL (OPLL group) and eight patients with cervical spondylotic myelopathy as a control (non-OPLL group). The ligamentum flava in OPLL patients showed no evidence of ossification at the time of harvesting. The clinical diagnosis, patient gender and age of the tissue samples used in this study are shown in Table 1. There was no significant difference in patient ages between OPLL (mean, 66.9 ± 6.9 years) and non-OPLL (mean, 65.9 ± 6.6 years).

2.2. Cell isolation and culture

MSCs were isolated as described in the literature [10]. Briefly, collected samples were washed with phosphate-buffered saline (PBS), minced and digested with 3 mg/ml collagenase (Type5; Sigma–Aldrich, St. Louis, MO, USA) in α-modified Eagle's medium (α-MEM; Invitrogen, Carlsbad, CA, USA) at 37 °C for 3 h. Nucleated cells were plated in plastic dishes (Nalge Nunc International, Rochester, NY, USA) at density of 5×10^5 cells/90-mm dishes. Cells were maintained in complete culture medium (α-MEM + 10% fetal bovine serum (FBS) (JRH Bioscience, Lenexa, KS, USA), 100 U/ml penicillin G sodium and streptomycin sulfate (Invitrogen)). Culture dishes were incubated in a humidified atmosphere of 95% air and 5% CO_2 at 37 °C for 14 days as passage 0.

2.3. Flow cytometric analysis and cell sorting

For flow cytometric analysis of cell surface antigens and cell sorting, MSCs were stained for the expression of CD34 and CD105 using a mouse anti-human CD34 antibody coupled with PE and a mouse anti-human CD105 antibody coupled with PerCP-Cy5.5, respectively (BD Biosciences, San Jose, CA, USA). Passage 1 cells (1×10^6 cells) were harvested and washed with PBS containing 2% FBS. Cells were suspended in 50 μl PBS containing specific antibodies and incubated for 45 min on ice. The cells were washed in PBS, filtered using a 35-μm strainer (BD Falcon), resuspended in 1 ml of PBS and analyzed using a FACSAria™ II instrument (BD Biosciences). For cell sorting, gates were defined as negative for CD34 ($CD34^-$) and positive for CD105 ($CD105^+$) according to the isotype control fluorescence intensity. Data were analyzed using BD FACSDiva™ software v6.1.3 (BD Biosciences).

Table 1
Clinical diagnosis, gender and age of tissue samples.

non-OPLL group		OPLL group	
Sex/age	Diagnosis	Sex/age	Diagnosis
F/56	CSM	M/53	C-OPLL, T-OLF
M/60	CSM	M/62	C-OPLL, T-OPLL, T-OLF
M/60	CSM	M/65	C-OPLL
M/60	CSM	F/67	C-OPLL, T-OPLL, T-OLF
M/71	CSM	M/71	C-OPLL, T-OLF
M/72	CSM	M/71	C-OPLL, T-OPLL, T-OLF
F/73	CSM	F/71	C-OPLL, T-OPLL
M/75	CSM	M/75	C-OPLL

M: male, F: female, CSM: cervical spondylotic myelopathy, C: cervical spine, T: thoracic spine, OPLL: ossification of the posterior longitudinal ligament of the spine, OLF: ossification of the ligamentum flavum of the spine.

2.4. Single cell cloning efficiency

Sorted cells at passage 1 were seeded in complete culture medium into two 96-well culture plates (Nalge Nunc International) per sample at a density of one cell per well by FACS. After 14 days of culture, wells were stained with 0.5% crystal violet (Wako Pure Chemical Industries, Osaka, Japan). Wells that reached 30 or more cells per well were counted as single-cell clones [12].

2.5. In vitro differentiation and histological analysis

2.5.1. Osteogenic differentiation

Sorted MSCs at passage 1 were seeded at densities of 100 cells/cm^2 for cytohistological staining and cultured at subconfluent levels. Osteogenic induction medium was then added for 21 days. Osteogenic induction medium consisted of complete culture medium supplemented with 1 nM dexamethasone (ICN Biomedicals Inc., Costa Mesa, CA, USA), 10 mM β-glycerol phosphate and 50 μg/ml ascorbic acid (Wako Pure Chemical Industries), as previously reported [13]. To evaluate the mineralized matrix, cells were fixed with 4% formaldehyde and stained with 1% Alizarin Red S (Sigma–Aldrich) for 10 min. The calcium-bound dye was extracted using 100 mM hexadecylpyridinium chloride monohydrate (Wako Pure Chemical Industries) and quantified at an optical density (OD) of 570 nm. The experiment was performed once with triplicate wells for each sample. ALP activity was measured at days 0, 7 and 14 using a LabAssay™ ALP kit (Wako Pure Chemical Industries) and standardized to whole protein content in the lysate according to the manufacturer's instructions. The experiment was performed once with duplicate wells for each sample.

2.5.2. Adipogenic differentiation

Cells from passage 2 were seeded at densities of 10,000 cells/cm^2. Upon reaching the appropriate subconfluent level, cells were incubated in adipogenic induction medium (complete culture medium supplemented with 100 nM dexamethasone, 0.5 mM isobutylmethylxanthine and 100 μM indomethacin (Sigma–Aldrich)) for 21 days, as previously reported [14]. To evaluate lipid vesicle formation, cells were fixed with 4% formaldehyde and stained with 0.3% Oil Red O for 20 min. The dye was extracted using 60% isopropanol and the OD was measured at 490 nm. The experiment was performed once with duplicate wells for each sample.

2.5.3. Chondrogenic differentiation

5×10^5 cells at passage 2 were centrifuged for 10 min at 450×g in a 15-mL polypropylene tube. The pellet was treated with chondrogenic induction medium for 21 days. Chondrogenic induction medium consisted of complete culture medium supplemented with 500 ng/ml bone morphogenetic protein (BMP) 2, 10 ng/ml transforming growth factor (TGF)-β3 (R&D Systems, Minneapolis, MN, USA) and 100 nM dexamethasone, as previously reported [10]. The pellets were evaluated in terms of diameter and pellet wet weight. The diameter was measured using ImageJ software (Rasband, WS, rsb.info.nih.gov/ij). The pellets were fixed in 10%

Table 2
List of primers used for real-time PCR.

Gene	Forward primer 5′–3′	Reverse primer 5′–3′
GAPDH	TGCACCACCAACTGCTAGC	GGCATGGACTGTGGTCATGAG
BMP2	AGATGAACACAGCTGGTCACAGA	GGAAGGATGCCCTTTTCCA
Runx2	GCCTTCAAGGTGGTAGCCC	CGTTACCCGCCATGACAGTA
ALP	ACGAGCTGAACAGGAACAACGT	CACCAGCAAGAAGAAGCCTTTG
Osteocalcin	TGAGAGCCCTCACACTCCTC	ACCTTTGCTGGACTCTGCAC
Osteopontin	CGCAGACCTGACATCCAGT	GGCTGTCCCAATCAGAAGG
PPARγ2	TGAATGTGAAGCCCATTGAA	CTGCAGTAGCTGCACGTGTT
LPL	ATGTGGCCCGGTTTATCA	CTGTATCCCAAGAGATGGACATT
Sox9	GTACCCGCACTTGCACAAC	TCGCTCTCGTTCAGAAGTCTC
COL2A1	CCGGGCAGAGGGCAATAGCAGGTT	CATTGATGGGGAGGCGTGAG
COL10A1	CATGTTTGGGTAGGCCTGTATAAGA	ACTCCCTGAAGCCTGATCCA

G3PDH: glyceraldehyde-3-phosphate dehydrogenase, BMP2: bone morphogenetic protein 2, Runx2: runt-related transcription factor 2, ALP: alkaline phosphatase, PPARγ2: peroxisome proliferator-activated receptor gamma 2, LPL: lipoprotein lipase, Sox9: sex-determining region Y-type high mobility group box 9, COL2A1: collagen type 2 alpha 1, COL10A1: collagen type 10 alpha 1.

formaldehyde, dehydrated through serial ethanol dilutions and embedded in paraffin. Blocks were cut into 5-μm sections and stained with Alcian Blue (Sigma–Aldrich). Images were captured on a light microscope (BX41; Olympus, Tokyo, Japan) and ImageJ software (Rasband) was used to quantify differences in Alcian Blue staining between samples. To standardize measurements, the ImageJ automatic thresholding routine was used to avoid bias introduced by an observer manually setting the imaging threshold. The Alcian Blue stained area of the pellet was quantified with the percentage of the positive area to the total area [15]. The experiment was performed once with duplicate pellets for each sample.

2.6. RNA isolation and Real-Time PCR analysis

The differences between the mRNA levels of osteogenic-, adipogenic- and chondrogenic-related genes in stem cell differentiation were analyzed using real-time PCR. Total RNA was extracted on days 0, 7, 14 and 21 of each induction periods using an RNeasy Mini Kit (QIAGEN, Valencia, CA, USA) according to the manufacturer's instructions. Real-time PCR was conducted using Power SYBR Green PCR Master Mix on an ABI Prism® 7000 Sequence Detection System (Applied Biosystems, Foster City, CA, USA). Specific primer pairs for each gene (Table 2) were designed using Primer Express software (Applied Biosystems). The expression level of each gene was normalized with that of the housekeeping gene, glyceraldehyde-3-phosphate dehydrogenase (GAPDH). Graphs show the relative expression levels compared with the control on day 0.

2.7. Statistical analysis

Data from eight samples in each group were used for statistical analyses, with the exception of chondrogenic-related gene expressions ($n = 5$ for each group). Data input and calculations were performed with SPSS ver.12.0 J (SPSS Inc., Chicago, IL, USA). All quantitative values are expressed as mean ± SEM. Experimental data between non-OPLL group and OPLL group were compared using Mann–Whitney *U*-test. Gene expression levels of each mRNA were compared between non-OPLL group and OPLL group on each day. $P < 0.05$ was considered statistically significant.

3. Results

3.1. Isolation and flow cytometric analysis of MSCs from spinal ligament

MSCs obtained from spinal ligaments were plastic-adherent and demonstrated characteristic spindle-shaped and fibroblast-like morphology in both OPLL and non-OPLL groups (Fig. 1A). Flow cytometric analysis was used to examine the proportions of $CD34^-/CD105^+$ cells, which is indicative of MSCs, in both groups (Fig. 1B). The percentages of $CD34^-/CD105^+$ passage-1 cells in non-OPLL and OPLL groups were 90.7 ± 4.5% and 89.6 ± 4.9%, respectively (Fig. 1C).

3.2. Single cell cloning efficiency

Passage 1 cells were seeded at a statistical density of one cell per well in 192 wells for each sample. After 14 days, colonies were stained with crystal violet. Single cell cloning efficiency was 48.3 ± 3.9 clones in non-OPLL group and 52.0 ± 8.9 clones in OPLL group per 192 wells (Fig. 1D).

3.3. In vitro differentiation and histological analyses

3.3.1. Osteogenesis

After 21 days in basal growth media, none of the MSC cultures showed evidence of spontaneous mineralization (Fig. 2A). However, under osteogenic induction medium, mineralization was observed in both OPLL and non-OPLL groups, with calcium deposition visualized by Alizarin Red S staining. To quantify the mineralized content, bound Alizarin Red S dye was dissolved and measured at 570 nm. The OD values were 1.9 ± 0.9 in the non-OPLL group and 13.1 ± 4.0 in the OPLL group (Fig. 2B), demonstrating a significant difference between the two groups ($P = 0.0117$). Furthermore, ALP activity on day 7 under the osteogenic conditions and day 14 under basal media and osteogenic induction media were significantly higher in the OPLL group as compared with those values in the non-OPLL group (Fig. 2C). This finding indicates that the osteogenic potential of MSCs derived from the ligaments of patients with OPLL is greater than that of MSCs derived from the ligaments of non-OPLL patients.

3.3.2. Adipogenesis

In basal growth conditions, MSCs from both OPLL and non-OPLL patients formed a monolayer, with no apparent spontaneous lipid vacuole formation (Fig. 3A). Following 21 days of adipogenic induction, light microscopy of Oil Red O-stained sections revealed the formation of lipid vacuoles in both groups. To quantify the staining intensity, bound Oil Red O dye was extracted and measured at 490 nm. The OD values were 0.30 ± 0.06 in the non-OPLL group and 0.27 ± 0.07 in the OPLL group (Fig. 3B).

3.3.3. Chondrogenesis

After 21 days of chondrogenic induction, MSCs from both groups formed semitranslucent pellets of an increased size owing

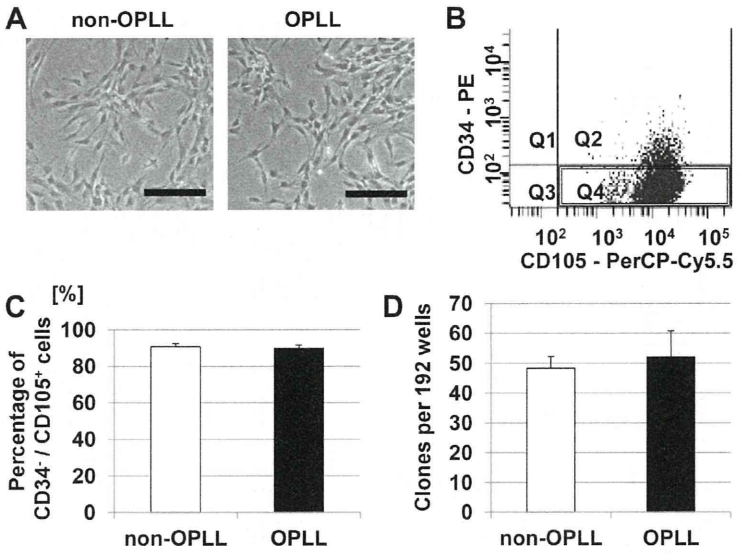

Fig. 1. (A) Phase contrast microscopic view of mesenchymal stem cells (MSCs) at passage 0. (B) Flow cytometric analysis of cell surface antigens. Cells inside the box (Q4) were negative for CD34 ($CD34^-$) and positive for CD105 ($CD105^+$). (C) Percentages of $CD34^-$ and $CD105^+$ cells. (D) Single cell cloning efficiency. Scale bars: 100 μm.

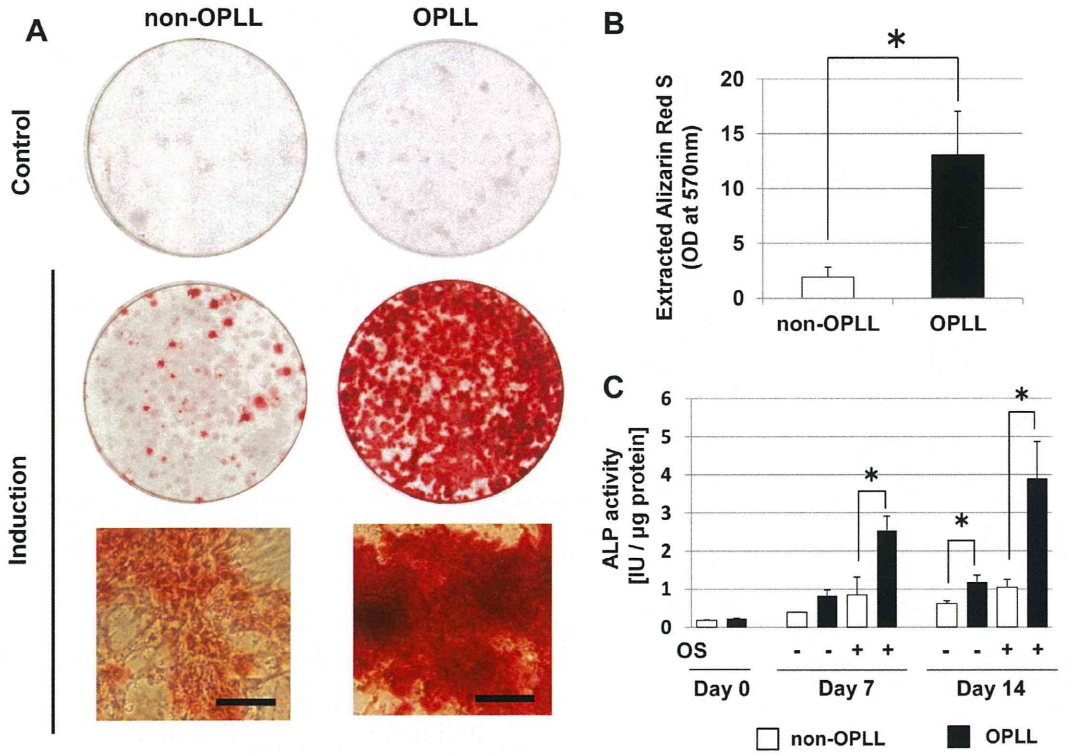

Fig. 2. Osteogenic differentiation potential. (A) Alizarin Red S staining was used to assess calcium deposition after 21 days in osteogenic induction medium. (B) Bound Alizarin Red S was dissolved and measured at 570 nm to quantify mineral content. (C) Alkaline phosphatase (ALP) activity was assessed at days 0, 7 and 14 under osteogenic induction media (OS+) and basal media (OS−). The *asterisk* indicates a significant difference; $P < 0.05$. Scale bars: 100 μm.

to production of extracellular matrix (Fig. 3C). Comparing the non-OPLL and OPLL groups, the diameters of pellets were 0.97 ± 0.07 mm and 0.99 ± 0.06 mm (Fig. 3E), and the weights were 0.49 ± 0.09 mg and 0.43 ± 0.05 mg (Fig. 3F), respectively. Pellets were then sectioned and stained with Alcian Blue to assess the degree of chondrogenesis between the groups. Alcian blue staining of pellets formed in basal medium was weak or negative, while clearly positive after 21 days in chondrogenic differentiation medium (Fig. 3D). Percentages of Alcian Blue staining per pellet were 42.7 ± 3.7% in the non-OPLL group and 38.3 ± 6.2% in the OPLL group (Fig. 3G).

3.4. Gene expression

The expression of osteogenic, adipogenic and chondrogenic-related genes during the course of lineage-specific differentiation

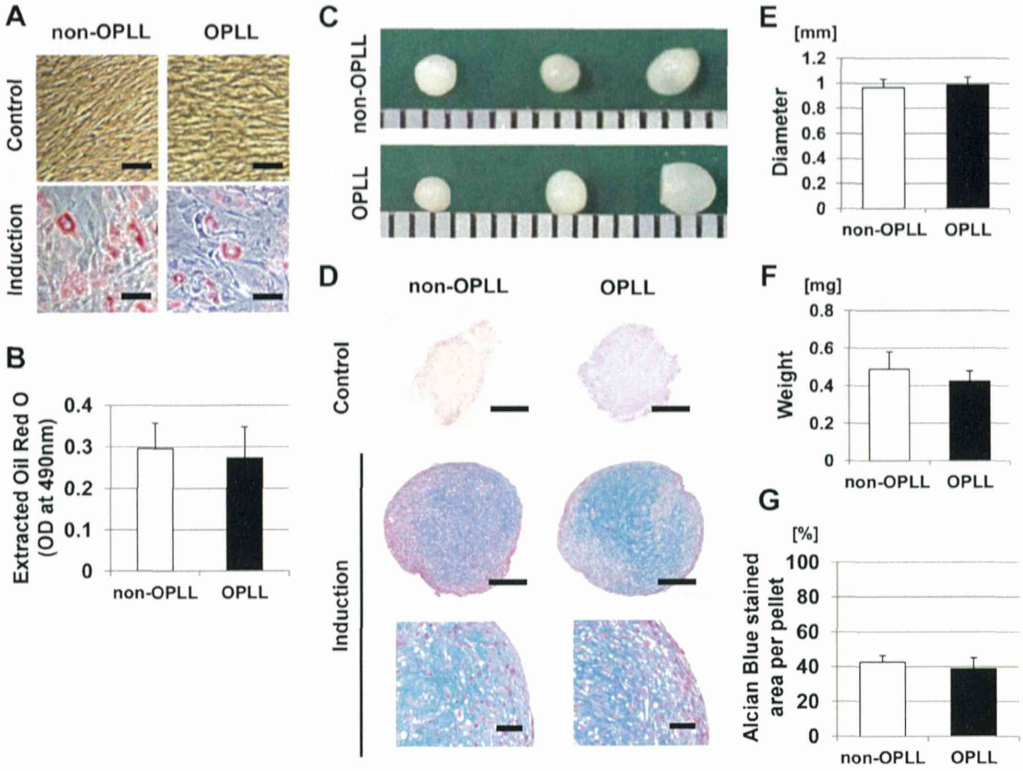

Fig. 3. Adipogenic and chondrogenic differentiation potential. (A) Oil Red O staining was used to assess lipid vacuole formation after 21 days in adipogenic induction medium. (B) Bound Oil Red O dye was extracted and measured the OD at 490 nm. Scale bars: 50 μm. (C) Representative pellet formation after 21 days culture in chondrogenic induction medium measured against a 0.5-mm scaled ruler. (D) Histological sections stained with Alcian blue. Scale bars: 200 μm. Higher magnifications of sections (Bottoms). Scale bars: 50 μm. (E) Diameter and (F) weight of the pellets were equivalent in cells from the two groups. (G) Percentages of Alcian Blue-positive areas per pellet.

was investigated. The mRNA levels of BMP2, Runx2, ALP, osteocalcin and osteopontin, known osteogenic markers, were all enhanced by osteogenic induction in both groups, as compared with expression in basal media (Fig. 4A–E; fold-change increase over control levels). In particular, BMP2 and ALP were higher in OPLL group than in the non-OPLL group at day 7, and Runx2 was higher on days 14 and 21 in OPLL group than in the non-OPLL group significantly. The mRNA levels of adipogenic markers PPARγ2 and LPL were also elevated under adipogenic conditions in both groups compared with control conditions (Fig. 4F and G). However, there were no significant differences in the expression of these two genes between the OPLL and non-OPLL groups under adipogenic conditions. Similarly, while the mRNA levels of the chondrogenic markers Sox9, COL2A1 and COL10A1 were elevated by chondrogenic induction, no significant difference was observed between OPLL and non-OPLL groups (Fig. 4H–J).

4. Discussion

In this study, we sought to assess the capacity of MSCs residing in the spinal ligament tissue to undergo lineage commitment. Using various assays, we clearly showed that MSCs harvested from the ligaments of patients with OPLL have an increased osteogenic differentiation potential as compared with MSCs from patients without evidence of ligament ossification. However, single cell cloning efficiency, adipogenic and chondrogenic differentiation potentials, and the expression levels of adipogenic- and chondrogenic-related genes were equivalent between the two groups. These results suggest that MSCs in the ligaments of patients with OPLL have a propensity toward becoming osteogenic cells.

As previously reported, one disadvantage of conventional MSC isolation techniques is the unavoidable contamination from hematopoietic and heterogeneous cells, including various progenitor and fibroblastic cells [16–18]. Indeed, the expression of CD34, a known hematopoietic cell marker, was small but not negligible because of this unavoidable contamination using the conventional method. $CD105^+$ cells have been reported to have a more homogeneous population of colony forming unit-fibroblasts and the capacity to form bone *in vivo* [19] as well as the potential to differentiate into cells of a chondrogenic lineage [20]. For these reasons, we selected $CD34^-/CD105^+$ cells from cells isolated by conventional MSC preparation for our experiments. From this point, cell sorting created a homogeneous population with which to rigorously evaluate the characteristics of MSCs.

Ectopic ossification is the process by which bone forms in soft tissues in response to injury, inflammation, or genetic diseases or through excess signaling, such as that which occurs when exogenous growth factors are supplemented at a wound site. However, despite numerous studies, the biological mechanism responsible for the development of ectopic ossification has not been fully elucidated. Perhaps the most extreme cases of ectopic ossification can be found in patients with FOP [21], which is induced by a combination of genetic mutations and acute inflammatory responses. Reportedly, aberrant stem cell differentiation can contribute to ectopic ossification in the onset of FOP as a result of activin-like kinase-2 mutations and the conversion of endothelial cells to cells of a mesenchymal-like phenotype [7]. In this study, the origin and localization of isolated MSCs in spinal ligament tissues was not determined, but one possibility is that MSCs were induced by through this mechanism of enhanced endothelial-mesenchymal conversion.

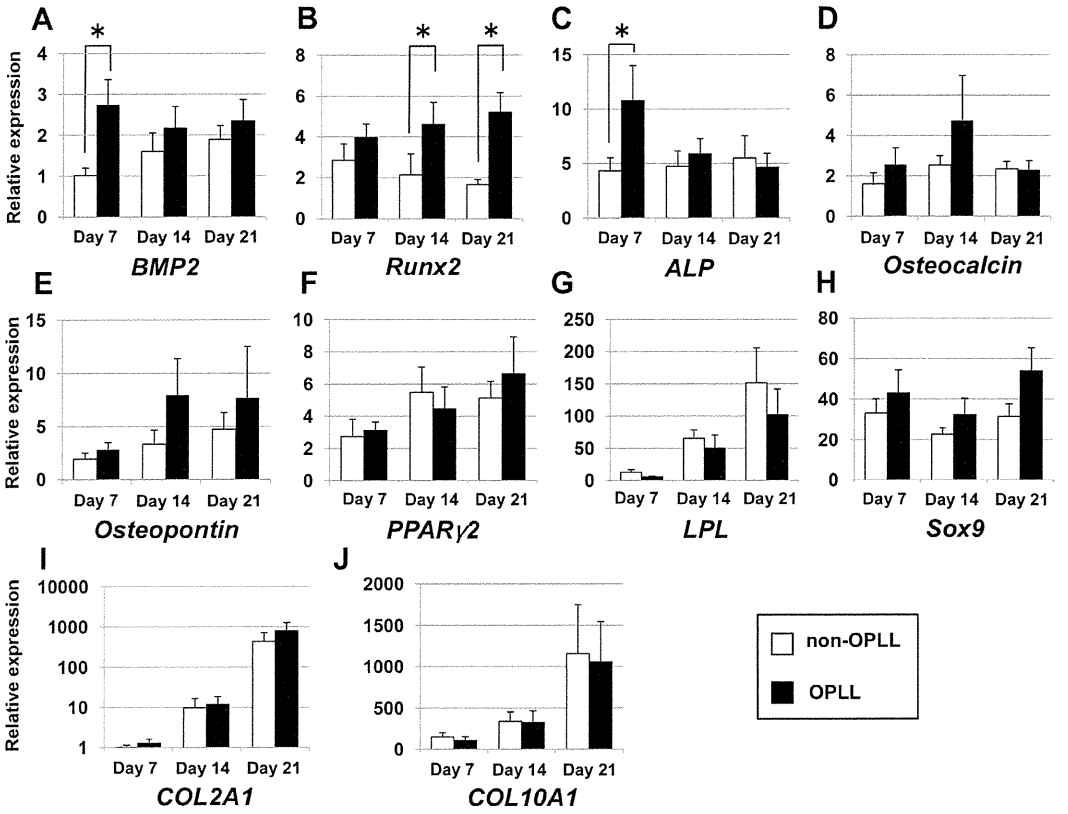

Fig. 4. Expression of osteogenic, adipogenic and chondrogenic genes. (A) BMP2, (B) Runx2, (C) ALP, (D) osteocalcin, and (E) osteopontin are osteogenic markers. (F) PPARγ2 and (G) LPL are adipogenic markers. (H) Sox9, (I) COL2A1 and (J) COL10A1 are chondrogenic markers. The *asterisk* indicates a significant difference between two groups at a particular each day; $P < 0.05$.

Putative osteoprogenitor cells have been identified by others in certain tissues such as traumatized muscle and aortic valves [9,22]. However, the process for the spontaneous phenotypic differentiation of MSCs into osteoprogenitor cells or osteoblasts has not been clearly elucidated. Some authors suggest that miRNA and epigenetic alterations regulate osteogenic differentiation of progenitor cells in muscle sites and *in vitro* [23,24]. We, too, hypothesize that genetic and epigenetics aspects are major factors controlling lineage commitment of MSCs.

One caveat of this study is that samples were harvested from non-ossified ligamentum flavum. However, as previously mentioned, OPLL patients have a tendency toward systemic ossification of numerous ligaments and soft tissues, thus it is likely that even MSCs obtained from non-ossified ligaments would exhibit the features of this pathological condition. There are some other limitations that should be noted. First, because of ethical reasons, control samples were not from healthy patients but from patients with cervical spondylotic myelopathy without evidence of ligament ossification. Second, this is an *in vitro* study. Some reports have suggested that *in vitro* mineral deposition does not correlate with *in vivo* bone formation [25,26]. Thus, this investigation should be followed up using an *in vivo* model to study the mechanism of osteogenic differentiation of MSCs that leads to ectopic ossification in a physiological system. Third, we used only two markers instead of more to sort the cell, as discussed above. And finally, the current study included a relatively limited number of tissue samples ($n = 8$) and is thus not adequately powered to perform all of the necessary statistical analyses.

In conclusion, this study indicates an increase in the osteogenic differentiation potential of MSCs from OPLL patients and the findings suggest that this propensity toward increased osteogenesis of these MSCs may be a causal factor for ossification in the ligaments of these patients.

Acknowledgments

This work was supported by a Grant-in-Aid from the Investigation Committee on Ossification of the Spinal Ligaments, the Public Health Bureau of the Japanese Ministry of Labour, Health and Welfare and by a Grant-in-Aid from the Ministry of Education, Culture, Sports, Science and Technology of Japan (Grants-in-Aid 24590310). We thank Drs. Kazumasa Ueyama, Naoki Echigoya, Akio Sannohe, Gentaro Kumagai, Takuya Numasawa, Kanichiro Wada, Toru Yokoyama, Kazunari Takeuchi, Shuichi Aburakawa, Yoshihito Yamasaki, Taisuke Nitobe, Kenji Kowatari and Takashi Tomita for their contributions to sample collection, and thank Medical Corporation Seijin Society Ono Hospital for financial support. We also thank Chikara Ohyama and Tohru Yoneyama of the Department of Urology, Hirosaki University Graduate School of Medicine for excellent technical assistance with flow cytometric analysis and cell sorting, and Kazuhiko Seya of the Department of Pharmacology, Hirosaki University Graduate School of Medicine for excellent technical assistance with ALP assay and valuable discussions.

References

[1] S. Matsunaga, M. Kukita, K. Hayashi, et al., Pathogenesis of myelopathy in patients with ossification of the posterior longitudinal ligament, J. Neurosurg. 96 (2002) 168–172.

[2] K. Furukawa, Pharmacological aspect of ectopic ossification in spinal ligament tissues, Pharmacol. Ther. 118 (2008) 352–358.

[3] M. Mochizuki, A. Aiba, M. Hashimoto, et al., Cervical myelopathy in patients with ossification of the posterior longitudinal ligament, J. Neurosurg. Spine 10 (2009) 122–128.
[4] W.R. Stetler, F. La Marca, P. Park, The genetics of ossification of the posterior longitudinal ligament, Neurosurg. Focus 30 (2011) E7.
[5] D. Resnick, S.R. Shaul, J.M. Robins, Diffuse idiopathic skeletal hyperostosis (*DISH*): Forestier's disease with extraspinal manifestations, Radiology 115 (1975) 513–524.
[6] P.D. Utsinger, Diffuse idiopathic skeletal hyperostosis, Clin. Rheum. Dis. 11 (1985) 325–351.
[7] D. Medici, E.M. Shore, V.Y. Lounev, et al., Conversion of vascular endothelial cells into multipotent stem-like cells, Nat. Med. 16 (2010) 1400–1406.
[8] E.R. Nelson, V.W. Wong, P.H. Krebsbach, et al., Heterotopic ossification following burn injury: the role of stem cells, J. Burn Care Res. 33 (2012) 463–470.
[9] J.H. Chen, C.Y. Yip, E.D. Sone, et al., Identification and characterization of aortic valve mesenchymal progenitor cells with robust osteogenic calcification potential, Am. J. Pathol. 174 (2009) 1109–1119.
[10] T. Asari, K. Furukawa, S. Tanaka, et al., Mesenchymal stem cell isolation and characterization from human spinal ligaments, Biochem. Biophys. Res. Commun. 417 (2012) 1193–1199.
[11] S. Chin, K. Furukawa, A. Ono, et al., Immunohistochemical localization of mesenchymal stem cells in ossified human spinal ligaments, Biochem. Biophys. Res. Commun. 436 (2013) 698–704.
[12] V. Dexheimer, S. Mueller, F. Braatz, et al., Reduced reactivation from dormancy but maintained lineage choice of human mesenchymal stem cells with donor age, PLoS One 6 (2011) e22980.
[13] Y. Sakaguchi, I. Sekiya, K. Yagishita, et al., Comparison of human stem cells derived from various mesenchymal tissues: superiority of synovium as a cell source, Arthritis Rheum. 52 (2005) 2521–2529.
[14] I. Sekiya, B.L. Larson, J.T. Vuoristo, et al., Adipogenic differentiation of human adult stem cells from bone marrow stroma (MSCs), J. Bone Miner. Res. 19 (2004) 256–264.
[15] S.J. Bruce, N.C. Butterfield, V. Metzis, et al., Inactivation of Patched1 in the mouse limb has novel inhibitory effects on the chondrogenic program, J. Biol. Chem. 285 (2010) 27967–27981.
[16] S. Morikawa, Y. Mabuchi, Y. Kubota, et al., Prospective identification, isolation, and systemic transplantation of multipotent mesenchymal stem cells in murine bone marrow, J. Exp. Med. 206 (2009) 2483–2496.
[17] Y. Jiang, B.N. Jahagirdar, R.L. Reinhardt, et al., Pluripotency of mesenchymal stem cells derived from adult marrow, Nature 418 (2002) 41–49.
[18] L. da Silva Meirelles, P.C. Chagastelles, N.B. Nardi, Mesenchymal stem cells reside in virtually all post-natal organs and tissues, J. Cell Sci. 119 (2006) 2204–2213.
[19] H. Aslan, Y. Zilberman, L. Kandel, et al., Osteogenic differentiation of noncultured immunoisolated bone marrow-derived CD105+ cells, Stem Cells 24 (2006) 1728–1737.
[20] M.K. Majumdar, V. Banks, D.P. Peluso, et al., Isolation, characterization, and chondrogenic potential of human bone marrow-derived multipotential stromal cells, J. Cell. Physiol. 185 (2000) 98–106.
[21] E.M. Shore, F.S. Kaplan, Insights from a rare genetic disorder of extra-skeletal bone formation, fibrodysplasia ossificans progressiva (FOP), Bone 43 (2008) 427–433.
[22] W.M. Jackson, A.B. Aragon, J.D. Bulken-Hoover, et al., Putative heterotopic ossification progenitor cells derived from traumatized muscle, J. Orthop. Res. 27 (2009) 1645–1651.
[23] T. Oishi, A. Uezumi, A. Kanaji, et al., Osteogenic differentiation capacity of human skeletal muscle-derived progenitor cells, PLoS One 8 (2013) e56641.
[24] Z. Li, C. Liu, Z. Xie, et al., Epigenetic dysregulation in mesenchymal stem cell aging and spontaneous differentiation, PLoS One 6 (2011) e20526.
[25] K.H. Larsen, C.M. Frederiksen, J.S. Burns, et al., Identifying a molecular phenotype for bone marrow stromal cells with in vivo bone-forming capacity, J. Bone Miner. Res. 25 (2010) 796–808.
[26] P. Janicki, S. Boeuf, E. Steck, et al., Prediction of in vivo bone forming potency of bone marrow-derived human mesenchymal stem cells, Eur. Cell Mater. 21 (2011) 488–507.